

Mechanistic Studies of the Reaction of Ir(III) Porphyrin Hydride with 2,2,6,6-Tetramethylpiperidine-1-oxyl to an Unsupported Ir–Ir Porphyrin Dimer

Siu Yin Lee,[†] Chi Wai Cheung,[†] I-Jui Hsu,^{*,‡} and Kin Shing Chan^{*,†}

[†]Department of Chemistry, The Chinese University of Hong Kong, Shatin, New Territories, Hong Kong, People's Republic of China, and [‡]Department of Molecular Science and Engineering, National Taipei University of Technology, Taipei 10608, Taiwan

Received July 7, 2010

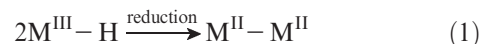
Reaction of hydrido[5,10,15,20-tetrakis(*p*-tolyl)porphyrinato]iridium(III) (Ir(tp)H) (**1**) with 2,2,6,6-tetramethylpiperidine-1-oxyl (TEMPO) (**2**) at room temperature gave a 90% yield of the unsupported iridium(II) porphyrin dimer, Ir^{II}₂(tp)₂ (**3**). Kinetic measurements revealed that the oxidation followed overall second-order kinetics: rate = $k[\text{Ir}(\text{tp})\text{H}][\text{TEMPO}]$, $k(25\text{ }^\circ\text{C}) = 6.65 \times 10^{-4}\text{ M}^{-1}\text{ s}^{-1}$. The entropy of activation ($\Delta S^\ddagger = -25.3 \pm 2.5\text{ cal mol}^{-1}\text{ K}^{-1}$) and the kinetic isotope effect of 7.2 supported a bimolecular associative mechanism in the rate-determining hydrogen atom transfer from Ir(tp)H to TEMPO.

Introduction

Unsupported iridium(II) complexes have drawn much interest from chemists due to their fundamental importance in basic chemical bonding, unique chemical reactivity, and potential industrial application as fuel cell catalysts.^{1–15} The Ir^{II}–Ir^{II} distances in these complexes can provide an experimental basis for a theoretical understanding of the nature of a metal–metal single bond.^{1,6,7,9,11–13} Iridium(II) porphyrin dimers (Ir^{II}₂(por)₂) are convenient sources of reactive metal-loradicals displaying unique organometallic reactions, such

as the 1,2-addition to olefins^{3,14} and benzylic carbon–hydrogen bond activation.¹⁰ The applications of an iridium(II) porphyrin dimer as an efficient electrochemical catalyst for the four-electron reduction of oxygen relevant to fuel cell technology have also been documented.^{2,15,16}

Unsupported iridium(II) metal bonded dimers, however, are relatively inaccessible with limited general synthetic methods available. Most syntheses are rather specialized in ligand types and experimental conditions. Some examples involve electrochemical¹ and chemical oxidation of Ir(I)^{11,12} complexes, chemical reduction of Ir(III),^{6,13} and prolonged photolysis of Ir(III) complexes.^{2,3,6}



We have reported the clean and high-yielding reaction of Ir^{III}(oep)H^{4,10} (oep = octaethylporphyrinato dianion) with 2,2,6,6-tetramethylpiperidine-1-oxyl (TEMPO) in benzene under nitrogen at room temperature to give Ir^{II}₂(oep)₂ as well as a related macrocyclic type complex (eq 1).⁸ This formal hydrogen atom transfer (HAT) or controlled reduction at ambient conditions can access both a rhodium(II) and iridium(II) porphyrin dimer as well as a sterically hindered Rh porphyrin monomer¹⁷ conveniently simply by the subsequent vacuum removal of the slight excess of TEMPO used and the coproduct 2,2,6,6-tetramethylpiperidine-1-hydroxyl (TEMPOH). No overoxidative degradation of air-sensitive metal(II) dimers occurs. Given the operational simplicity of this general synthesis of M^{II}–M^{II} with supporting macrocyclic

*To whom correspondence should be addressed. E-mail: ksc@cuhk.edu.hk (K.S.C.).

- (1) Rasmussen, P. G.; Anderson, J. E.; Bailey, O. H.; Tamres, M.; Bay, J. C. *J. Am. Chem. Soc.* **1985**, *107*, 279–281.
- (2) Collman, J. P.; Kim, M. K. *J. Am. Chem. Soc.* **1986**, *108*, 7847–7849.
- (3) Del Rossi, K. L.; Wayland, B. B. *J. Chem. Soc., Chem. Commun.* **1986**, 1653–1655.
- (4) Chan, K. S.; Leung, Y. B. *Inorg. Chem.* **1994**, *33*, 3187.
- (5) Heinekey, D. M.; Fine, D. A.; Harper, T. G. P.; Michel, S. T. *Can. J. Chem.* **1995**, *73*, 1116–1125.
- (6) Heinekey, D. M.; Fine, D. A.; Barnhart, D. *Organometallics* **1997**, *16*, 2530–2538.
- (7) Hückstidt, H.; Homborh, H. Z. *Anorg. Allg. Chem.* **1997**, *623*, 369–378.
- (8) Feng, M.; Chan, K. S. *Organometallics* **2002**, *21*, 2743–2750.
- (9) Villarroya, B. E.; Tejel, C.; Rohmer, M.-M.; Oro, L. A.; Ciriano, M. A.; Benard, M. *Inorg. Chem.* **2005**, *44*, 6536–6544.
- (10) Cheung, C. W.; Chan, K. S. *Organometallics* **2008**, *27*, 3043–3055.
- (11) Patra, S. K.; Rahaman, S. M. W.; Majumdar, M.; Sinha, A.; Bera, J. K. *Chem. Commun.* **2008**, *22*, 2511–2513.
- (12) Huang, H.; Rheingold, A. L.; Hughes, R. *Organometallics* **2009**, *28*, 1575–1578.
- (13) Lee, H.-P.; Hsu, Y.-F.; Chen, T.-R.; Chen, J.-D.; Chen, K. H.-C.; Wang, J.-C. *Inorg. Chem.* **2009**, *48*, 1263–1265.
- (14) (a) For properties of Ir^{II} porphyrin, see: Zhai, H.; Bunn, A.; Wayland, B. *Chem. Commun.* **2001**, 1294–1295. (b) Cui, W.; Li, S.; Wayland, B. B. *J. Organomet. Chem.* **2007**, *692*, 3198–3206.
- (15) Collman, J. P.; Chng, L. L.; Tyvoll, D. A. *Inorg. Chem.* **1995**, *34*, 1311–1324.

(16) Shi, C.; Mak, K. W.; Chan, K. S.; Anson, F. C. *J. Electroanal. Chem.* **1995**, *397*, 321–324.

(17) Chan, K. S.; Li, X. Z.; Dzik, W. I.; de Bruin, B. J. *Am. Chem. Soc.* **2008**, *130*, 2051–2061.

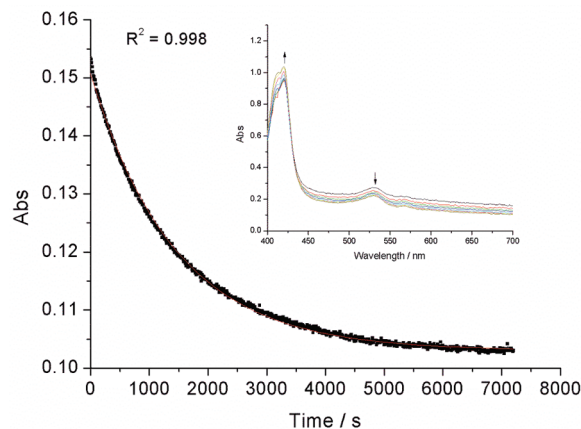
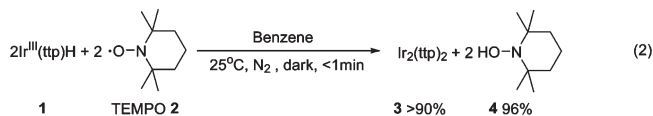


Figure 1. First-order absorbance decay. (Inset) Wavelength scan of the reaction between Ir(tp)H and TEMPO.

ligands and the current interest in HAT,¹⁸ we have applied this method to the readily available Ir^{III}(tp)H¹⁰ (tp = 5,10,15,20-tetrakis(*p*-tolyl)porphyrinato dianion) to produce Ir^{II}₂(tp)₂.¹⁰ We now report the results of the mechanistic studies based on a kinetic investigation of this formal hydrogen atom transfer reaction from a transition metal hydride bond to an oxygen centered radical.

Results and Discussions

Stoichiometry. Ir₂(tp)₂ (**3**) was prepared by the reaction of Ir(tp)H (**1**) with TEMPO (**2**) (eq 2). The clean and high yielding formation of >90% yield of Ir₂(tp)₂¹⁹ from the Ir(tp)H solution in benzene-*d*₆ occurred within a minute upon the addition of a slight excess of TEMPO (1.1 equiv) at room temperature and was accompanied by an instantaneous color change from brown to deep brown. The diagnostic Ir₂(tp)₂ in the ¹H NMR signal at δ (pyrrole) = 8.33 ppm with the complete disappearance of the Ir(tp)–H signal at –53.6 ppm consolidated the complete transformation. The ¹H NMR spectrum remained clean at room temperature after 1 day but slowly showed small amounts of impurity signals after 2 days.²⁰ Any secondary reaction of Ir₂(tp)₂ with TEMPO or TEMPOH would be slow and minor at room temperature within 2 days and would not interfere with subsequent kinetic studies.



To gain a mechanistic understanding of the Ir₂(tp)₂ formation, the reaction order of Ir(tp)H and TEMPO

(18) For a leading reference, see: Wu, A.; Mader, E. A.; Datta, A.; Hrovat, D. A.; Borden, W. T.; Mayer, J. M. *J. Am. Chem. Soc.* **2009**, *131*, 11985–11997.

(19) Preliminary solid state EXAFS studies revealed Ir–Ir distance = 2.69 Å, typical of an Ir^{II}–Ir^{II} bond length. The fitted coordination geometry showed a five-coordinated (H₂O) Ir(tp) fragment in contrast with the Ir(tp) fragment elucidated from the ¹H NMR data taken in benzene-*d*₆. We rationalized that the water ligand does not exchange rapidly in the solid state while it undergoes dynamic exchange in benzene solution and appears as a broad baseline signal in ¹H NMR.

(20) Possible decomposition processes are the carbon–hydrogen and carbon–carbon bond activations of TEMPO by Ir^{II}(tp) formed via dissociation from Ir₂(tp)₂. See ref 17.

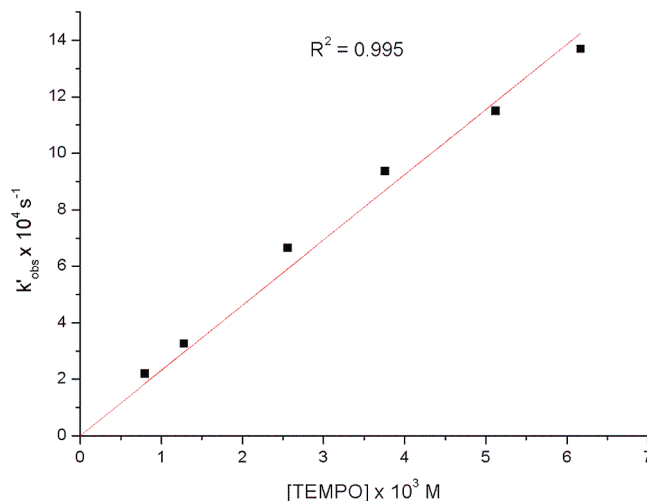


Figure 2. Linear variation of rate constant with TEMPO (25 °C).

Table 1. *k'*_{obs} under Different TEMPO and Ir(tp)H Concentrations at 25 °C

Entry	[Ir(tp)H] ₀ × 10 ⁵ M	[TEMPO] ₀ × 10 ³ M	<i>k'</i> _{obs} × 10 ⁴ s ^{−1}	Error × 10 ⁶ s ^{−1}
1	2.49	2.56	6.70	5.32
2	13.0	2.56	6.81	4.01
3	5.41	0.80	2.20	2.15
4	5.41	1.28	3.26	7.20
5	5.41	2.56	6.65	5.33
6	5.41	3.76	9.37	7.31
7	5.41	5.12	11.5	5.49
8	5.41	6.17	13.7	8.67

were evaluated by kinetic measurements made spectrophotometrically by following changes in the absorbance at 530 nm at 25 °C (Figure 1). Initial concentrations of TEMPO (7.99 × 10^{−4}–6.17 × 10^{−3} M) were maintained to be at least in a 10-fold excess compared to Ir(tp)H (2.49 × 10^{−5}–1.30 × 10^{−4} M) to ensure pseudo-first-order conditions. All the reactions were monitored for at least 4 half-lives.

With excess TEMPO, the observed rate constants *k*_{obs} at 25 °C (eq 3, Table 1) were evaluated by a good first-order exponential fitting of the absorbance changes (Figure 1). The values do not change with a greater than 5-fold change of [Ir(tp)H] (Table 1, entries 1–2), and the first-order dependency of [Ir(tp)H] is established. At constant initial [Ir(tp)H], the *k'*_{obs} values obey a linear relationship with a nearly 8-fold change of [TEMPO] (Table 1, entries 3–8; Figure 2) and establish a first-order dependency on TEMPO. The overall rate law is shown in eq 3 where *k*_{obs} = 0.231 M^{−1} s^{−1} at 25.0 °C. The slope of the plot (*k*_{obs}) was then evaluated to be 0.231 M^{−1} s^{−1}. The overall second-order kinetics suggest a bimolecular reaction of [Ir(tp)H] with [TEMPO].

$$\text{rate} = k_{\text{obs}}[\text{TEMPO}][\text{Ir}(\text{tp})\text{H}] \quad (3)$$

$$k'_{\text{obs}} = k_{\text{obs}}[\text{TEMPO}] \quad (4)$$

To evaluate the activation parameters, the temperature-dependent observed rate constants *k'*_{obs} were measured from 15 to 50 °C (eq 4, Table 2), sufficiently low enough to

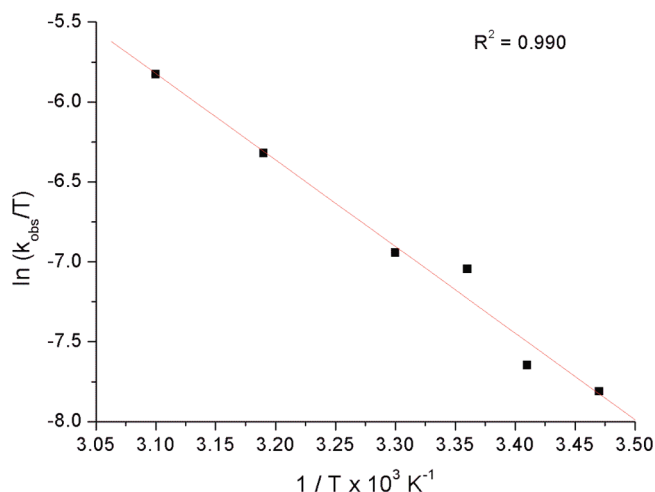


Figure 3. Eyring plot of the reaction between Ir(tp)H and TEMPO.

Table 2. Temperature Effect on Observed Rate Constant

T (°C)	T (K)	$1/T$ ($\times 10^{-3} \text{ K}^{-1}$)	k'_{obs} ($\times 10^{-4} \text{ s}^{-1}$)	Error of k'_{obs} ($\times 10^{-6} \text{ s}^{-1}$)	k_{obs} ($\text{M}^{-1} \text{ s}^{-1}$)	\ln - (k_{obs}/T)
15.0	288	3.47	2.993	3.0256	0.1169	-7.809
20.0	293	3.41	3.513	4.7661	0.1372	-7.645
25.0	298	3.36	6.650	2.4855	0.2598	-7.045
30.0	303	3.30	7.492	4.7661	0.2926	-6.942
40.0	313	3.19	14.42	2.3293	0.5633	-6.320
50.0	323	3.10	24.37	2.0077	0.9520	-5.827

ensure clean $\text{Ir}_2(\text{tp})_2$ formation and stability without side reactions which were ascertained by the same final absorbance in all runs. The linear Eyring plot shown in Figure 3 is evaluated to yield the following activation parameters: $\Delta H^\ddagger = 10.7 \pm 0.8 \text{ kcal mol}^{-1}$; $\Delta S^\ddagger = -25.3 \pm 2.5 \text{ cal mol}^{-1} \text{ K}^{-1}$, and $\Delta G^\ddagger = 18.3 \pm 2.6 \text{ kcal mol}^{-1}$. From the small magnitude of ΔH^\ddagger , neither bond breaking nor bond formation dominates in the rate-determining step; the reaction likely proceeds in a concerted manner. The negative and typical magnitude of ΔS^\ddagger indicates an associative, bimolecular reaction, in line with the second-order kinetics.

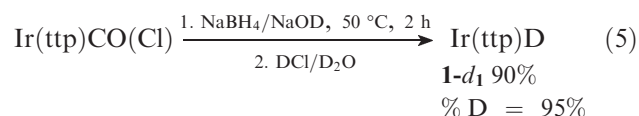
The above findings suggest a rate-determining hydrogen atom transfer from Ir(tp)H to TEMPO in the transition state of the dehydrogenative dimerization reaction. To test whether HAT is the rate-determining step and to elucidate the geometry of the transition state, the kinetic isotope effects (KIEs) were measured. We then synthesized Ir(tp)D (95% Ir-D) by the reduction of Ir(tp)(CO)Cl with $\text{NaBH}_4/\text{NaOD}$ followed by deuteration with D_2O (eq 5). The rate constants of the reactions were then measured at 25 and 50 °C and yielded the KIEs 7.2 and 6.8, respectively (Table 3). The KIEs show a slight decrease at 50 °C due to the Arrhenius behavior.^{21,22} The KIEs are, however, very large for a reaction involving a transition metal–hydride bond cleavage.²² The reported Ir(oep)–H stretching frequency²⁴ at 2343 cm^{-1} can be used to estimate the theoretical maximum

Table 3. Observed Rate Constant k'_{obs} of Ir(tp)D

Entry	Temperature (°C \pm 0.2)	k'_{obs} (s^{-1}) ^a	k'_{obs} of Ir(tp)H at the same T	KIE
1	25.0	9.27×10^{-5} $\pm 2.92 \times 10^{-7}$	6.65×10^{-4} $\pm 2.49 \times 10^{-6}$	7.2 ± 0.1
2	50.0	3.59×10^{-4} $\pm 2.64 \times 10^{-6}$	24.37×10^{-4} $\pm 2.01 \times 10^{-6}$	6.8 ± 0.1

^a Corrected according to the ratio of H/D in starting material.

primary KIE value 5.3 for a three-center model.²⁵ We do not understand the origin of the large KIEs though a tunneling effect has been suggested.²³ Nonetheless, the high KIE values around 7 are supportive of the rate-determining cleavage of the Ir–H bond in the transition state.



Based on the above data, Scheme 1 illustrates the proposed mechanism of the overall reaction. The rate-determining hydrogen atom transfer reaction from (tp)–Ir–H to the oxygen center of TEMPO most likely occurs in a bimolecular manner in the transition state to give TEMPOH and $\text{Ir}^{\text{II}}(\text{tp})$. $\text{Ir}^{\text{II}}(\text{tp})$ then undergoes rapid self-dimerization to produce $\text{Ir}_2(\text{tp})_2$.

Precoordination of TEMPO cis or trans to Ir(tp)H prior to the Ir–H cleavage is not likely.²⁶ The sterically more accessible trans-coordination of TEMPO to Ir(tp)H would require a second-order dependency of TEMPO which is not consistent with the observed rate law. Alternatively, this trans-TEMPO–Ir(tp)H could undergo tunneling in the HAT step. In view of the small KIEs and very little temperature effect as well as the structural difficulty of this HAT through an iridium porphyrin core, the trans coordination mode is unlikely and not productive. The alternative cis-coordination of TEMPO to the Ir(tp)–H, while consistent with the rate law, was not observed under the conditions of measurement as no saturation kinetics on TEMPO were observed.²⁶

The hydrogen transfer could occur via a two-step process: electron transfer–proton transfer (ET/PT) or alternative electron transfer–hydride transfer (ET/HT) or a one-step hydrogen atom transfer. For the ET/PT process, an iridium porphyrin hydride cation radical and TEMPO anion intermediate would form. The first oxidation potential of the more electron-rich Ir(oep)Pr (the oxidation potential of Ir(tp)H is unknown) in CH_2Cl_2 has been measured to be 0.65 V vs SCE,²⁷ and the reduction potential of TEMPO is -1.241 V vs SCE.²⁸ The lowest activation barrier is therefore $\sim 0.6 \text{ V}$. While we do not have direct evidence to completely rule out the possibility of an ET/PT process, several lines of reasons would suggest that this process is less favorable or

(21) Kwart, H. *Acc. Chem. Res.* **1982**, *15*, 401–408.

(22) Denny, M. C.; Smythe, N. A.; Cetto, K. L.; Kemp, R. A.; Goldberg, K. I. *J. Am. Chem. Soc.* **2006**, *128*, 2508–2509.

(23) Bakac, A. *J. Am. Chem. Soc.* **1997**, *119*, 10726–10731.

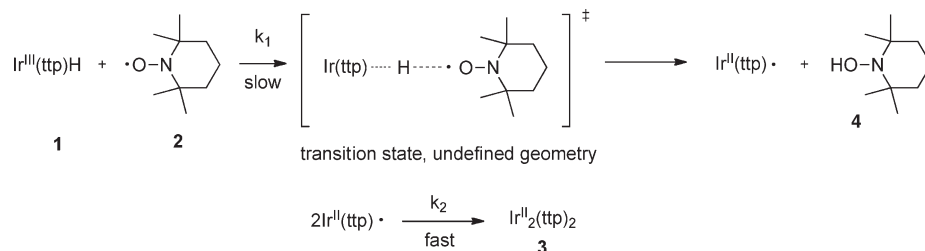
(24) Farnos, M. D.; Woods, B. A.; Wayland, B. B. *J. Am. Chem. Soc.* **1986**, *108*, 3659–3663.

(25) Espensen, J. H. *Chemical Kinetics and Reaction Mechanisms*, 2nd ed.; McGraw-Hill: New York, 1995; p 214.

(26) Marder, E. A.; Mayer, J. M. *Inorg. Chem.* **2010**, *49*, 3685–3687.

(27) Kadish, K. M.; Cornillon, J.-L.; Mitaine, P.; Deng, Y. J.; Korp, J. D. *Inorg. Chem.* **1989**, *28*, 2534–2542.

(28) Hodgson, J. L.; Namazian, M.; Bottle, S. E.; Coote, M. L. *J. Phys. Chem. A* **2007**, *111*, 13595–13605.

Scheme 1. Proposed Mechanism for Dehydrogenative Dimerization of Ir(tp)H with TEMPO

experimentally difficult to test and therefore not economical. (1) ET/PT processes of a hydrogen transfer reaction occur in polar solvents such as CH_2Cl_2 , CH_3CN , and water.^{29–31} The Ir(tp)–H reaction is only feasible in a nonpolar benzene solvent. A reaction carried out in THF- d_8 gave complex mixtures and does not allow the solvent effect study. (2) A light-induced charge-transfer process can favor the ET/PT in a highly absorbing metalloporphyrin species but was experimentally minimized as much as possible by carrying out all the reactions in NMR tubes wrapped with aluminum foil for room light protection. (3) The addition of salt has been reported to allow the direct spectral observation of short-lived charged intermediates in manifesting the ET/PT process.²⁹ This approach is not applicable in benzene solvent since it dissolves salts sparingly. (4) While an external base can enhance the PT rate, the decomposition of $\text{Ir}_2(\text{tp})_2$ by a base, ligand, or coordinating solvent through disproportionation does not allow the base effect study.^{14a,32} Therefore, the reaction mechanism cannot be probed by the solvent effect. While it may be helpful that further steric^{31,33} and electronic modifications³⁴ of both Ir porphyrin H and nitroxide can aid to distinguish the HAT and ET/PT pathways, we currently favor the HAT pathway as the simplest mechanism to account for the kinetic data.³¹ For the electron transfer ET/HT process, an Ir(tp)H anion radical and an N-oxo ammonium ion intermediates would form. The reported first reduction potential of Ir(oep)Pr (–1.88 V vs SCE)²⁷ and oxidation potential of TEMPO (0.638 V)³⁵ can yield a minimum barrier of 1.2 V which is much higher than the observed ΔH^\ddagger ($10.7 \pm 0.8 \text{ kcal mol}^{-1}$) and can be ruled out convincingly.

Conclusions

A mechanistic investigation by kinetics has been carried out for the reaction between Ir(tp)H and the nitroxide radical, TEMPO, in benzene to give $\text{Ir}_2(\text{tp})_2$. The rate equation was found to follow overall second-order kinetics: $\text{rate} = k_{\text{obs}}[\text{Ir}(\text{tp})\text{H}][\text{TEMPO}]$. The observed activation parameters ($\Delta H^\ddagger = 10.7 \pm 0.8 \text{ kcal mol}^{-1}$; $\Delta S^\ddagger = -25.3 \pm 2.5 \text{ cal}$

$\text{mol}^{-1} \text{ K}^{-1}$; $\Delta G^\ddagger = 18.3 \pm 2.6 \text{ kcal mol}^{-1}$) support that the reaction operates by a bimolecular associative pathway. The kinetic isotope effect for the reaction further supports that the Ir–H bond cleavage occurs in the rate-determining step.

Experimental Section

General Procedures. All materials were obtained from commercial suppliers and used without further purification unless otherwise specified. Benzene was distilled from sodium under nitrogen. Tetrahydrofuran (THF) was freshly distilled from sodium benzophenone ketyl under nitrogen prior to use. 2,2,6,6-tetramethyl-piperidine-1-oxyl (TEMPO) was obtained from Aldrich and was purified by vacuum sublimation. Ir(tp)–Cl(CO)¹⁰ and Ir(tp)H¹⁰ were prepared according to the literature procedures. All solutions used were degassed thrice by a freeze–thaw–pump cycle and stored in a Teflon screwhead stoppered flask.

Preparation of Deutero(5,10,15,20-tetrakis(*p*-tolyl)porphyrinato)-iridium(III) [Ir(tp)D] (1-*d*₁). Ir(tp)D (1-*d*₁) was prepared according to the literature procedure for the synthesis of Ir(tp)H.¹¹ A suspension of Ir(tp)Cl(CO) (35.0 mg, 0.038 mmol) in THF (10 mL) and a solution of NaBH₄ (5.3 mg, 0.14 mmol) in aqueous NaOD (in D₂O) (1.0 M, 1.0 mL) were purged with N₂ for 15 min separately. Concentrated DCl (1 mL) (commercially available) was degassed for three freeze–thaw–pump cycles in a Teflon screw-capped tube. The solution of NaBH₄ was added slowly to the suspension of Ir(tp)Cl(CO) via a cannula. The mixture was heated at 70 °C under N₂ for 2 h in a Teflon screw-capped 250 mL round-bottomed flask to give a deep brown suspension. The mixture was then cooled in an ice–water bath under N₂, and DCl solution was added via a cannula. Under N₂, the reaction mixture was stirred in an ice–water bath until a dark brown precipitate formed and degassed water (200 mL) was then added to precipitate out the solid. The dark brown precipitate was collected under N₂ by suction filtration and washed with water to give 1-*d*₁ (31.3 mg, 0.034 mmol, 90%). ¹H NMR (C₆D₆, 400 MHz) δ –57.5 (s, 0.05 H, % D = 95%), 2.40 (s, 12 H), 7.21 (d, 4 H, *J* = 7.5 Hz), 7.36 (d, 4 H, *J* = 7.8 Hz), 7.92 (d, 4 H, *J* = 6.6 Hz), 8.20 (d, 4 H, *J* = 7.9 Hz), 8.81 (s, 8 H). The deuterium content of Ir(tp)D was found to be 95% using the residual Ir–H peak and the pyrrole signal as the internal standard for integration.

Reaction of Ir(tp)H and TEMPO. A Teflon screw-capped NMR tube was flushed with N₂ for 3 times. Ir(tp)H (1) (4.2 mg, 0.005 mmol) and degassed benzene-*d*₆ (0.5 mL) were added to the NMR tube under N₂ to form a homogeneous solution, and the solution was degassed for three freeze–thaw–pump cycles. 2,2,6,6-Tetramethylpiperidinoxy (TEMPO) (2) (1.1 mg, 0.007 mmol) was added under N₂ to the reaction mixture to form a homogeneous solution, and the tube was then flame-sealed under vacuum. Ir₂(tp)₂ (3) (90% NMR yield) was estimated by ¹H NMR spectroscopy using residual benzene as an internal standard. The coproduct TEMPOH (4) (96% NMR yield) was characterized and estimated by ¹H NMR spectroscopy using

(29) Bockman, T. M.; Hubig, S. M.; Kochi, J. K. *J. Am. Chem. Soc.* **1998**, *120*, 2826–2830.

(30) Schlesner, C. J.; Amatore, C.; Kochi, J. K. *J. Am. Chem. Soc.* **1984**, *106*, 3567–3577.

(31) Yiu, D. T. Y.; Lee, M. F. W.; Lam, W. W. Y.; Lau, T.-C. *Inorg. Chem.* **2003**, *42*, 1225–1232.

(32) Wayland, B. B.; Balkus, K. J., Jr.; Farnos, M. D. *Organometallics* **1989**, *8*, 950–955.

(33) Matsuo, T.; Mayer, J. M. *Inorg. Chem.* **2005**, *44*, 2150–2158.

(34) For electronic modification, Rh(tmp)H reacts with TEMPO to give Rh^{II}(tmp); see ref 17.

(35) Rychnovsky, S. D.; Vaidyanathan, R.; Beauchamp, T.; Lin, R.; Farmer, P. J. *J. Org. Chem.* **1999**, *64*, 6745–6749.

tetrakis(trimethylsilyl)silane as an internal standard. ^1H NMR (C_6D_6 , 400 MHz) δ 1.14 (s, 12 H), 1.29 (s, 2 H), 1.38 (s, 4 H), 1.53 (s, 1 H).

Kinetic Studies on Reaction of Ir(tp)H and TEMPO. Kinetic studies were carried out in the temperature range $(20.0\text{--}50.0) \pm 0.2$ °C. UV–visible time scans were carried out on a UV–vis spectrometer equipped with a temperature controller. The stock benzene solutions of TEMPO (0.019 mL, 7.680×10^{-2} M) and Ir(tp)H (0.415 mL, 3.248×10^{-4} M) were transferred respectively to the side arm and bottom of a Telfon-stopped Schlenk UV cell with a gastight syringe under N_2 carefully. Dried benzene (2.60 mL) was then transferred under N_2 to the same cell using a gastight syringe. The solutions were stirred for 10 min at 25.0 ± 0.2 °C inside the sample compartment under N_2 . The two stock solutions in the side arm and bottom of the UV cell respectively were mixed just before the absorbance was

measured. The reaction was monitored at 530 nm for 4–5 half-lives.

Kinetics Study of the Reaction between Ir(tp)D and TEMPO.

A stock solution of Ir(tp)D (**1-d₁**) in anhydrous benzene was prepared by dissolving Ir(tp)D (1.4 mg, 1.624×10^{-3} mmol) in degassed benzene in a 5.00 mL volumetric flask flushed with nitrogen. The stock solution was transferred to a Telfon screw-capped tube for degassing under N_2 , to give the brownish orange Ir(tp)D solution for UV analysis (3.248×10^{-4} M). Time scans were carried out at 25.0 and 50.0 (± 0.2) °C using the same concentrations of Ir(tp)H and TEMPO. The experimental procedures were similar to those for the kinetic studies of the reaction between Ir(tp)H and TEMPO.

Acknowledgment. We thank the Research Grants Council (No. 400308) of the HKSAR, China, for financial support.